Available online at www.sciencedirect.com

ScienceDirect

Ceramics International 40 (2014) 2359–2364

CERAMICS INTERNATIONAL

www.elsevier.com/locate/ceramint

Facile synthesis and performance of polypyrrole-coated hollow Zn_2SnO_4 boxes as anode materials for lithium-ion batteries

Ke Wang, Ying Huang*, Tiaozheng Han, Yang Zhao, Haijian Huang, Lele Xue

Department of Applied Chemistry and The Key Laboratory of Space Applied Physics and Chemistry, Ministry of Education, School of Science, Northwestern Polytechnical University, Xi'an 710072, PR China

Received 12 July 2013; received in revised form 30 July 2013; accepted 1 August 2013
Available online 19 August 2013

Abstract

Polypyrrole-coated hollow Zn_2SnO_4 boxes (hollow Zn_2SnO_4@PPY nanocomposites) had been prepared by a microemulsion polymerization. The structural, morphological and electrochemical properties were methodically investigated by means of XRD, TGA, BJH (pore size distribution analysis), SEM, TEM, and electrochemical measurements. Results show that the hollow Zn_2SnO_4 boxes with the uniform and cube like structure are coated by PPY. Electrochemical measurement suggests that hollow Zn_2SnO_4@PPY composites exhibit better cycling properties and lower initial irreversible capacities as anode materials for lithium-ion batteries. At a current density of 60 mA/g in the voltage about 0.01–3.0 V, the first discharge–charge capacities of hollow Zn_2SnO_4@PPY composites are 1105.2 mAh/g and 556 mAh/g. After 50 cycles, a specific charge capacity of 478.4 mAh/g remained and the coulombic efficiency reaches 98.2%, revealing better capacity retention compared with hollow Zn_2SnO_4 boxes.

Keywords: Hollow structure; Zn_2SnO_4; PPY coating; Lithium battery; Anode materials

1. Introduction

With the rapid development of electronic products, the increasing demands for both higher energy density and power density of batteries impelled investigators to develop new materials for lithium-ion batteries [1,2]. Sn-based materials [3–5], alloys [6–10], and transition-metal oxides [11–13] have been deemed as promising negative electrode materials for LIBs because of their high specific capacity, which are much higher than that of currently used graphite-based anodes ($\approx$ 370 mAh/g) [11,14]. As a kind of tin–zinc composite oxide, Zn_2SnO_4 is an essential material with high electron mobility, high electrical conductivity [15] and synergistic flame retardants [16]. These outstanding properties enable its applications in advanced technologies including solar cells [15], gas sensors [17], photocatalysts [18], and lithium ion batteries [19].This material, however, suffers from a rapid capacity fade due to the large volume changes upon Li-insertion/extraction processes as anode material.

To overcome such an expansion problem, considerable approaches have been attempted, and among the various methods, the hollow mesoscale structure is more attractive, whose mechanism makes use of the free volume in the hollow structure to cushion the volume changes [20–22]. In addition, conducting polymers can also improve the electrode properties and provide double buffer structures for the active materials [23].

In this report, we present a novel pathway to synthesize the hollow Zn_2SnO_4@PPY composites. Monomer pyrrole was polymerized by the emulsion polymerization method in the presence of these hollow Zn_2SnO_4 boxes, to prepare hollow Zn_2SnO_4@PPY composites. The hollow mesoscale structure and the addition of polypyrrole create a double buffer structure for Zn_2SnO_4. The hollow Zn_2SnO_4@PPY composites show the superior electrochemical performance than the original materials.

2. Experimental

2.1. Sample preparation

The hollow Zn_2SnO_4 boxes were synthesized based on our previous research, which are prepared via an alkali etching

*Corresponding authors. Tel.: +86 29 88431636.
E-mail addresses: wangke81554944@gmail.com (K. Wang), yingh@nwpu.edu.cn (Y. Huang).

0272-8842/$ - see front matter © 2013 Elsevier Ltd and Techna Group S.r.l. All rights reserved.
http://dx.doi.org/10.1016/j.ceramint.2013.08.006

method from the solid $ZnSn(OH)_6$ cubes [24]. The hollow Zn_2SnO_4@PPY composites were synthesized by a microemulsion polymerization way [25,26]. Firstly, the monomer pyrrole (the molar ratio of pyrrole to Zn_2SnO_4 was 2:1) was added into the flask with the solution of $C_{18}H_{29}SO_3Na$ (0.1 g) and the pH value was adjusted to 1–2. Then Zn_2SnO_4 and N-butanol (0.2 ml) were added into the solution with stirring for 1 h to form microemulsion. Subsequently, $(NH_4)_2S_2O_8$ water solution (the molar ratio of APS to pyrrole was 1:1) was slowly dropped into the liquid and the reaction was maintained under ice–water conditions for 12 h. The emulsion was broken by isopyknic acetone and the resulting composite was washed several times by HCl solution, deionized water and ethanol, and then dried at 60 °C under vacuum to obtain the hollow Zn_2SnO_4@PPY composites.

2.2. Materials characterization

The structures of the prepared samples were characterized by X-ray diffraction analysis (XRD) (Rigaku, model D/max-2500 system at 40 kV and 100 mA of Cu Kα). The surface morphology of the composites were performed by a model Tecnai F30 G2 (FEI Co., USA) field emission transmission electron microscope (FETEM) and a scanning electron microscope (SEM, VEGA 3, The Czech Republic, TESCAN). Thermal analysis of the composite was performed by thermal gravimetric analysis (TGA) (Model Q50, TA, USA) under an air atmosphere, with a heating rate of 20 °C/min, and the temperature range was from 20 to 800 °C.

Electrochemical performance was evaluated by a CR2016-type coin cell with a multi-channel current static system Land (LAND CT200IA). The anode electrodes were prepared by coating slurries consisting of Zn_2SnO_4@PPY composites (65 wt%) with acetylene black (15 wt%) and PVDF (20 wt %) as a binder dissolved in 1-methyl-2-pyrrolidinone (NMP) solution on a copper foil. Li foil was used as counter electrode, polypropylene (PP) film (Celgard 2400) as separator. The electrolyte was a solution of 1 M $LiPF_6$ in a mixture of ethylene (EC), dimethyl carbonate (DMC) and diethyl carbonate (DEC) (1:1:1, v/v/v). Cyclic voltammetry (CV) was

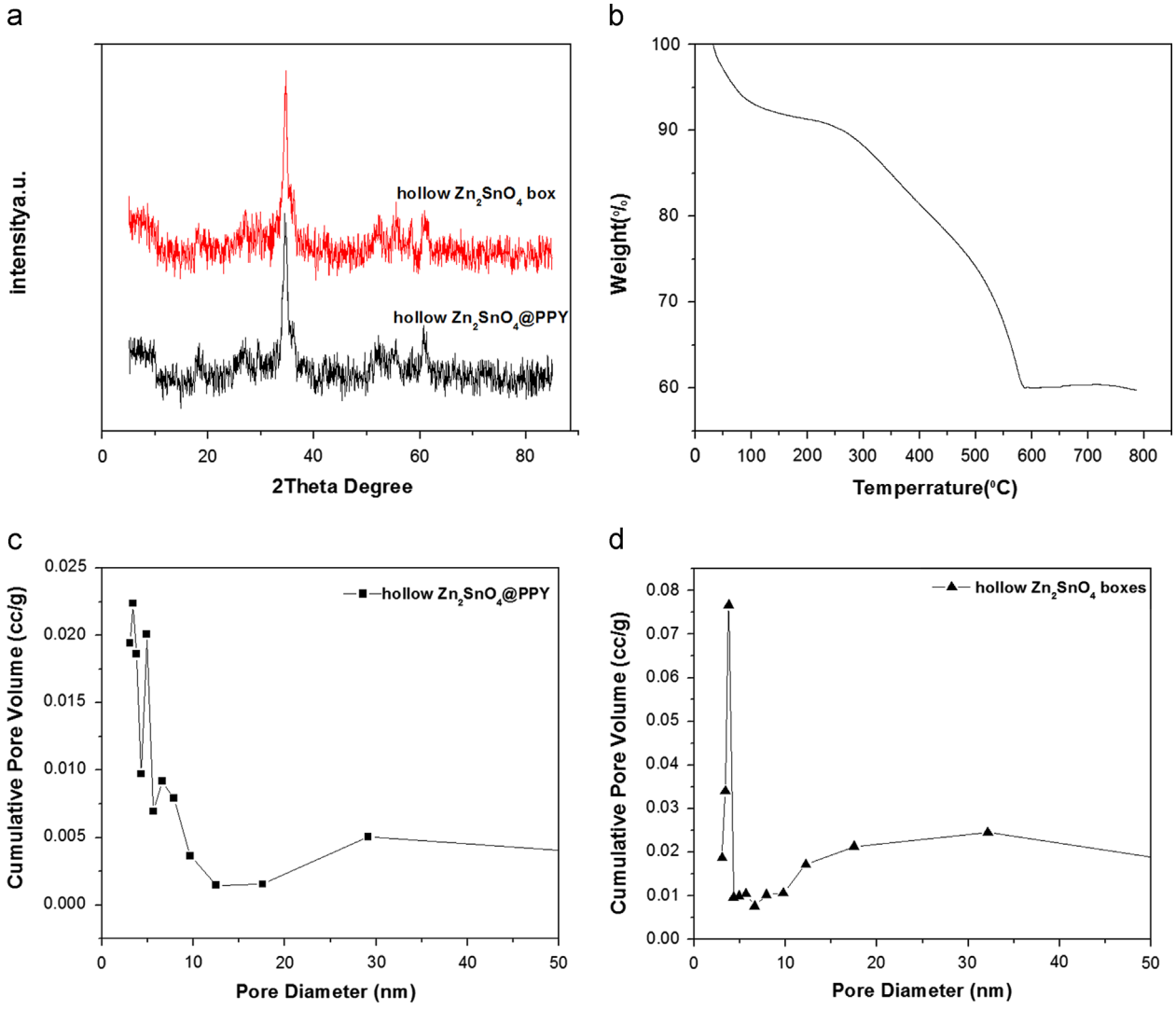

Fig. 1. XRD patterns of hollow Zn_2SnO_4 boxes and hollow Zn_2SnO_4@PPY (a), the TGA curve of hollow Zn_2SnO_4@PPY composites (b), the pore size distribution of hollow Zn_2SnO_4@PPY composites based on BJH method (c), and the pore size distribution of hollow Zn_2SnO_4 boxes composites based on the BJH method (d).

performed on a Series G 750™ Redefining Electrochemical Measurement (USA GMARY Co.).

3. Results and discussion

The crystal structures of the as-prepared samples are determined by XRD measurement. Fig. 1(a) shows the XRD patterns of hollow Zn_2SnO_4 boxes and hollow Zn_2SnO_4@PPY composites. All the diffraction peaks of the two samples are corresponding well with the data of pure phase of the inverse spinel Zn_2SnO_4 with lattice constants $a=8.657$ Å, $b=8.657$ Å, and $c=8.657$ Å (PDF #24-1470). The diffraction peaks of PPY cannot be detected in Fig. 1(a), which suggests it's little content and non-crystalline structure. There is an obvious peak at 26°corresponding to the (110) plane of the SnO_2 that fit to the reaction mechanism. The calcined reaction mechanism may be described as follows:

$$ZnSn(OH)_6 = Zn_2SnO_4 + SnO_2 + 6H_2O \ (T=700\ ^\circ C) \quad (1)$$

To investigate the weight loss of the hollow Zn_2SnO_4@PPY composites, TGA analysis has been carried out in air. Fig. 1(b) shows the TGA curves of the hollow Zn_2SnO_4@PPY composites. The weight loss before 100°C is attributed to the release of the absorbed water. An obvious weight loss occurs between 100 °C and 600 °C, indicating the decomposition of PPY in air. Therefore, the change in weight before and after the oxidation of PPY can be transformed into the amount of PPY in the materials. As can be seen from the TGA curves, the mass fraction of PPY in the Zn_2SnO_4@PPY composite is about 28 wt%

Fig. 1(c and d) shows the nitrogen adsorption–desorption isotherm and pore diameter distribution of hollow Zn_2SnO_4 boxes and hollow Zn_2SnO_4@PPY composites. The Barrett–Joyner–Halenda (BJH) pore size distribution analysis shows that the pore with more abundant diameter between hollow Zn_2SnO_4 boxes (3.7779 nm) and hollow Zn_2SnO_4@PPY composites(3.3921, 4.2983, and 4.9255 nm), indicating the composites have more mesoporous and large bore diameter. Thus, the porous structure of the composites is a benefit for lithium intercalation and de-intercalation, which also can provide a high conductive medium for electron transfer.

Fig. 2(a and b) shows the SEM image and TEM image of the as-prapared hollow Zn_2SnO_4 boxes, respectively. Both of them reveal that the pure boxes are smooth and each box is monodispersed. Fig. 2(c and d) shows the SEM images of hollow Zn_2SnO_4@PPY composites. Compared with the pure boxes, after PPY coating, there is no apparent change in the box structure although their surface becomes slightly rougher. From the TEM images of the Zn_2SnO_4@PPY composites (e and f), the outer surfaces of the boxes are covered with amorphous aggregated PPY. The thickness of the PPY layer was about 10 nm. The PPY coating can be the buffering materials in the charge/discharge process, which plays the double effect to alleviate the volume expansion of hollow Zn_2SnO_4 boxes.

The lithium storage capacity and cyclability of as anode in lithium ion cells were determined via galvanostatic charge/discharge cycling. Fig. 3(a) shows the discharge–charge curves in the first two cycles and the cycling performances of hollow Zn_2SnO_4@PPY composites. The voltage window is set between 0.01 V and 3.0 V and the current density is 60 mA/g. Results

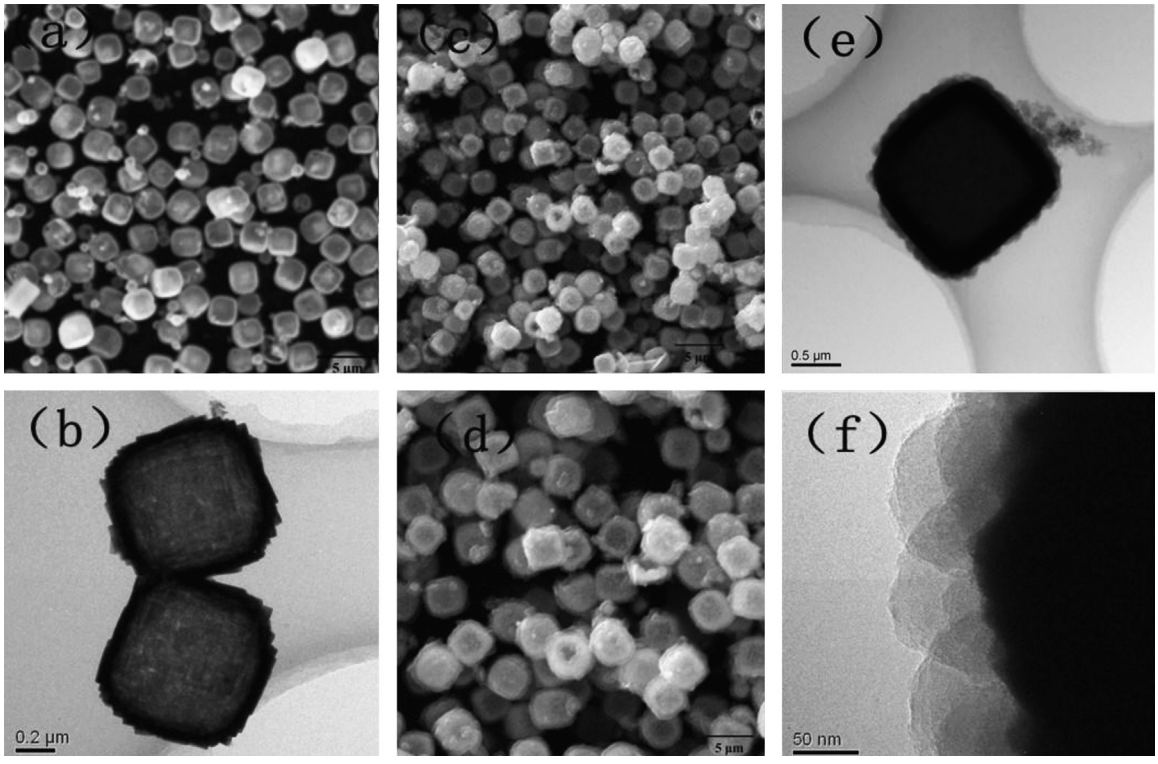

Fig. 2. SEM and TEM images of hollow Zn_2SnO_4 boxes and hollow Zn_2SnO_4@PPY composites.

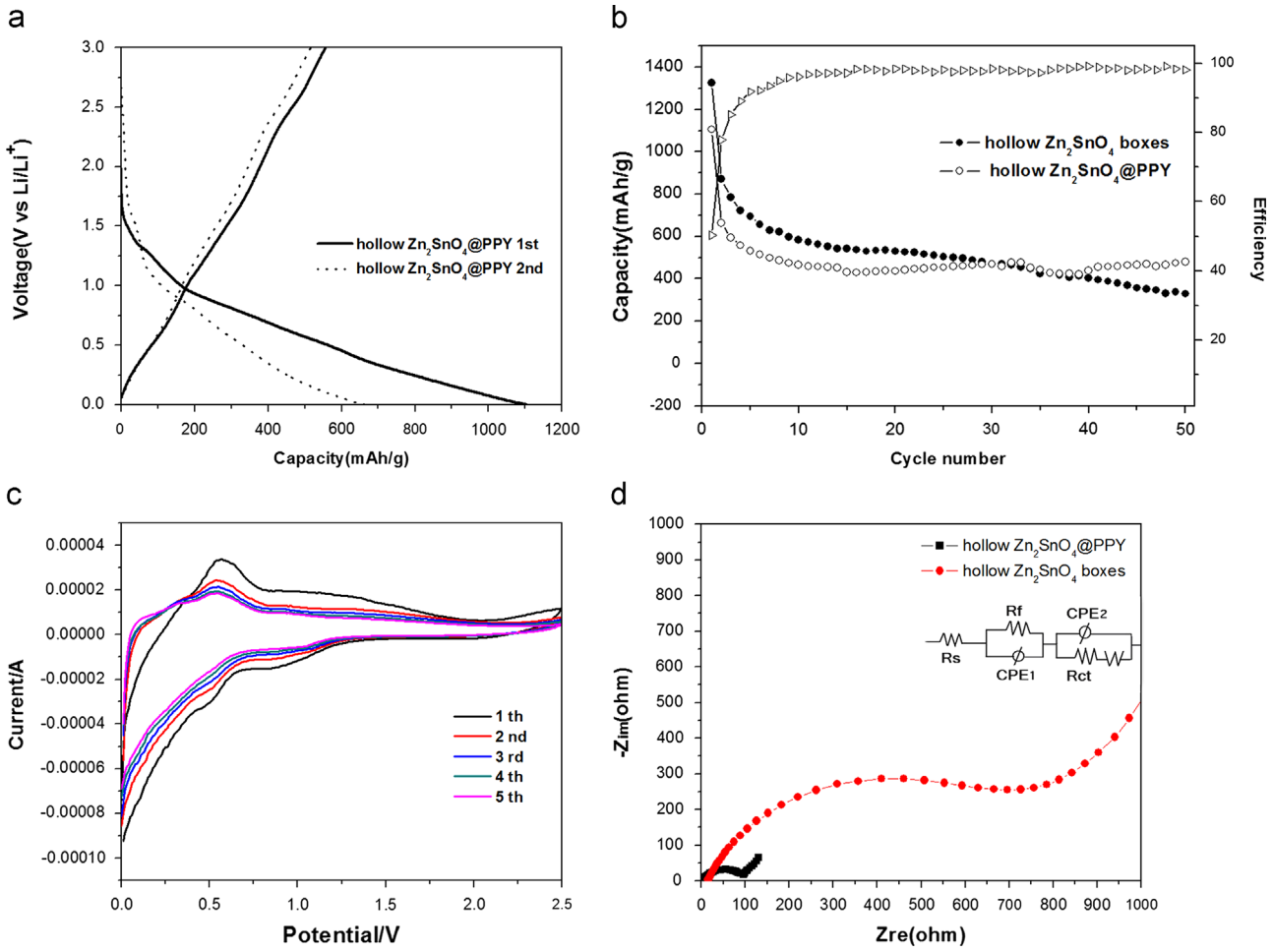

Fig. 3. (a) The discharge–charge curves of hollow Zn_2SnO_4@PPY composites for the first two cycles; (b) comparative cycling performance of hollow Zn_2SnO_4 boxes with hollow Zn_2SnO_4@PPY composites; (c) cyclic voltammetry of hollow Zn_2SnO_4@PPY composites; and (d) EIS of the hollow Zn_2SnO_4@PPY composites and hollow Zn_2SnO_4 boxes before cycling, including the equivalent circuit model of the studied system.

show that the first discharge–charge capacities of the hollow Zn_2SnO_4@PPY composites are 1105.2 mAh/g and 556 mAh/g. The irreversible capacity loss is 549.2 mAh/g with a coulombic efficiency of 50.3%. According to the mechanism of Zn_2SnO_4 during charge/discharge processes, the theoretical initial capacity of Zn_2SnO_4 is 803.7–1145.7 mAh/g and theoretical irreversible capacity is 342–684 mAh/g (theoretical reversible capacity 462 mAh/g), for the two possible reactions between Zn_2SnO_4 and Li-ion in the discharge process of the first cycle, as shown in Eqs. (2) and (3) [24]. The initial irreversible capacities of hollow Zn_2SnO_4@PPY composites are lower than those of Zn_2SnO_4, we believe the capacity fading of the composites can be partly attributed to the intercalation effect, and the theoretical reversible capacity of polypyrrole is low. In the 2nd cycle, the charge–discharge capacities reach 662.6 mAh/g and 516 mAh/g with a coulombic efficiency over 77.8% (Fig. 3(b)), beginning with the third cycle, the coulombic efficiency has been stabilized and approaches 95%. The large irreversible discharge capacity after the first cycle is gone away due to the side reaction with the electrolyte to form Li_2O and SEI film. Generally, the discharge capacity of the 1st cycle exceeds the theoretical capacity because of irreversible electrochemical reactions.

The comparison of the cycling performance between hollow Zn_2SnO_4 boxes and hollow Zn_2SnO_4@PPY composites is shown in Fig. 3(b). After 50 cycles, the reversible capacity of hollow Zn_2SnO_4@PPY composites retains 478.4 mAh/g at a current density of 60 mA/g, and the hollow Zn_2SnO_4 boxes retain only 328 mAh/g. The rapid fading of the hollow Zn_2SnO_4 boxes may result from the poor kinetics of electrochemical conversion reaction. The results indicate that the structure of the composites show the synergistic properties, the amorphous PPY in the hollow Zn_2SnO_4@PPY composites may buffer the large volume change of Zn_2SnO_4 boxes during Li^+ insertion/extraction and cracking of the composite electrode, and exhibit an improved cycling stability compared with hollow Zn_2SnO_4 boxes.

CV measurement was carried out to further clarify the origin of electrochemical capacity of the hollow Zn_2SnO_4@PPY composites in detail. Fig. 3(c) presents the first five complete cycles. It can be seen that, two cathodic peaks are observed at 0.23 V and 0.65 V, corresponding to the multi-step electrochemical lithiation process (Eqs. (2) and (3)). Meanwhile, two main anodic peaks are located near 1.37 V and 0.81 V, corresponding to the multi-step delithiation process. In addition, the anodic

peaks at 0.5 V and 1.5 V can be considered to be the de-alloying process of Li_xSn and Li_yZn (Eqs. (4) and (5)). The cathodic peaks at 0.26 V and 0.80 V may be the reversible reaction of whole process (Eqs. (4) and (5)).

$$4Li^+ + Zn_2SnO_4 + 4e^- = Sn + 2Li_2O + 2ZnO$$

$$8Li^+ + Zn_2SnO_4 + 8e^- = 2Zn + Sn + 4Li2O$$

$$xLi^+ + Sn + xe^- = Li_xSn \ (0 \le x \le 4.4)$$

$$yLi^+ + Zn + ye^- = Li_yZn \ (y \le 1) \quad (5)$$

To further evaluate the diffusion of lithium ion in the samples, Fig. 3(d) shows EIS analysis of the electrodes of the hollow Zn_2SnO_4@PPY composites and hollow Zn_2SnO_4 boxes at 0.5 V from 0.01 Hz to 100 kHz after 50 cycles. The impedance curves consist of one semicircle in the medium frequency region and an inclined line in the low-frequency region. Both the impedance plots can be fitted by the equivalent circuit diagram. In the equivalent circuit diagram, R_s is the electrolyte resistance, R_f is the SEI resistance, W is the Warburg impedance related to the diffusion of lithium-ions into the bulk of the electrode materials, CPE1 and CPE2 are two constant phase elements associated with the interfacial resistance and charge–transfer resistance, respectively. R_{ct} is the charge–transfer resistance [27,28]. Obviously, the R_{ct} of the hollow Zn_2SnO_4@PPY composites is significantly smaller than that of hollow Zn_2SnO_4 boxes, which indicates a smaller electrochemical reaction resistance because PPY can improve the electronic contact among the active particles. Therefore, the facts confirm that the electrode conductivity can be greatly increased by the PPY addition.

4. Conclusions

In summary, the hollow Zn_2SnO_4@PPY composites have been synthesized by a microemulsion polymerization way. Compared with the original boxes, Zn_2SnO_4@PPY composites exhibit improved structural stability and cycling performance. The amorphous PPY in the composites can provide free space to buffer the release of the stress caused by the drastic volume variation during the Li–Sn alloying/de-alloying process because of its highly dispersion, high conductivity and soft structure, which further improve the utilization of the hollow Zn_2SnO_4 boxes.

Acknowledgments

This work was supported by the Spaceflight Foundation of the People's Republic of China under Grant no. NBXW0001, the Spaceflight Innovation Foundation of China under Grant no. NBXT0002, the Basic Research Foundation of Northwestern Polytechnical University under Grant no. JC201269 and the Graduate Starting Seed Fund of Northwestern Polytechnical University No. Z2013146.

References

[1] M. Armand, J.M. Tarascon, Building better batteries, Nature 451 (2008) 652.
[2] B. Kang, G. Ceder, Battery materials for ultrafast charging and discharging, Nature 458 (2009) 190.
[3] L. Jose Tirado, Inorganic materials for the negative electrode of lithium-ion batteries: state-of-the-art and future prospects, Materials Science and Engineering 40 (2003) 103–136.
[4] N. Sharma, K.M. Shaju, G.V. Subba Rao, B.V.R. Chowdari, Anodic behaviour and X-ray photoelectron spectroscopy of ternary tin oxides, Journal of Power Sources 139 (2005) 250.
[5] L. Noerochim, J.Z. Wang, S.L. Chou, D. Wexler, H.K. Liu, Free-standing single-walled carbon nanotube/SnO_2 anode paper for flexible lithium-ion batteries, Carbon 50 (2012) 1289–1297.
[6] P.P. Ferguson, M.L. Martine, R.A. Dunlap, J.R. Dahn, Structural and electrochemical studies of $(Sn_xCo_{1-x})\ ^{60}C_{40}$ alloys prepared by mechanical attriting, Electrochimica Acta 54 (2009) 4534.
[7] R.A. Huggins, Lithium alloy negative electrodes, Journal of Power Sources 81–82 (1999) 13.
[8] C.F. Han, Q. Liu, D.G. Ivey, Nucleation of Sn and Sn–Cu alloys on Pt during electrodeposition from Sn–citrate and Sn–Cu–citrate solutions, Electrochimica Acta 54 (2009) 3419.
[9] X.Y. Fan, F.S. Ke, G.Z. Wei, L. Huang, S.G. Sun, Sn–Co alloy anode using porous Cu as current collector for lithium ion battery, Journal of Alloys and Compounds 476 (2009) 70.
[10] Z.B. Sun, X.D. Wang, X.P. Li, M.S. Zhao, Y. Li, Y.M. Zhu, X.P. Song, Electrochemical properties of melt-spun Al–Si–Mn alloy anodes for lithium-ion batteries, Journal of Power Sources 182 (2008) 353.
[11] Y. Idota, T. Kubota, A. Matsufuji, Y. Maekawa, T. Miyasaka, Tin-based amorphous oxide: a high-capacity lithium-ion-storage material, Science 276 (1997) 1395.
[12] P. Poizot, S. Laruelle, S. Grugeon, L. Dupont, J.M. Tarascon, Nano-sized transition-metal oxides as negative-electrode materials for lithium-ion batteries, Nature 407 (2000) 496.
[13] L. Kavan, K. Kratochvilova, M. Gratzel, Study of nanocrystalline TiO_2 (anatase) electrode in the accumulation regime, Journal of Electroanalytical Chemistry 394 (1995) 93.
[14] J.S. Chen, X.W. Lou, SnO_2-based nanomaterials: synthesis and apllication in lithium-ion batteries, Small 9 (2013) 1877–1893, http://dx.doi.org/10.1002/smll.201202601.
[15] B. Tan, E. Toman, Y.G. Li, Y.Y. Wu, Zinc stannate (Zn_2SnO_4) dye-sensitized solar cells, Journal of the American Chemical Society 129 (2007) 4162.
[16] A. Petsom, S. Roengsumran, A. Ariyaphattanakul, P. Sangvanich, An oxygen index evaluation of flammability for zinc hydroxystannate and zinc stannate as synergistic flame retardants for acrylonitrile–butadiene–styrene copolymer, Polymer Degradation and Stability 80 (2003) 17.
[17] J. Yu, G. Choi, Current–voltage characteristics and selective CO detection of Zn_2SnO_4 and ZnO/Zn_2SnO_4, SnO_2/Zn_2SnO_4 layered-type sensors, Sensors and Actuators B 72 (2001) 141–148.
[18] Y. Lin, S. Lin, Luo M. Liu, Enhanced visible light photocatalytic activity of Zn_2SnO_4 via sulfur anion-doping, Materials Letters 63 (2009) 1169–1171.
[19] A. Rong, X. Gao, G. Li, T. Yan, H. Zhu, J. Qu, et al., Hydrothermal synthesis of Zn_2SnO_4 as anode materials for Li-ion battery, Journal of Physical Chemistry B 110 (2006) 14754–14760.
[20] D.Y. Chen, G. Ji, Y. Ma, J.Y. Lee, J.M. Lu, Graphene-encapsulated hollow Fe_3O_4 nanoparticle aggregates as a high-performance anode material for lithium ion batteries, ACS Applied Materials and Interfaces 3 (2011) 3078–3083.
[21] W.M. Zhang, J.S. Hu, Y.G. Guo, S.F. Zheng, L.S. Zhong, W.G. Song, L.J. Wan, Tin-nanoparticles encapsulated in elastic hollow carbon spheres for high-performance anode material in lithium-ion batteries, Advanced Materials 20 (2008) 1160–1165.
[22] X.W. Lou, Y. Wang, C.L. Yuan, J.Y. Lee, L.A. Archer, Template-free synthesis of SnO_2 hollow nanostructures with high lithium storage capacity, Advanced Materials 18 (2006) 2325–2329.

[23] L. Yuan, J. Wang, S.Y. Chew, J. Chen, Z.P. Guo, L. Zhao, K. Konstantinov, H.K. Liu, Synthesis and characterization of SnO_2–polypyrrole composite for lithium-ion battery, Journal of Power Sources 174 (2007) 1183–1187.

[24] Y. Zhao, Y. Huang, Q. Wang, K. Wang, M. Zong, L. Wang, W. Zhang, X. Sun, Preparation of hollow Zn_2SnO_4 boxes for advanced lithium-ion batteriesRSC Advances, 3 (2013) 14480–14485, http://dx.doi.org/10.1039/C3RA42176G.

[25] Q.F. Wang, Y. Huang, J. Miao, Y. Zhao, Y. Wang, Synthesis and properties of Li_2SnO_3/polyaniline nanocomposites as negative electrode material for lithium-ion batteries, Applied Surface Science 258 (2012) 9896–9901.

[26] Ying Huang, Qiufen Wang, Yan Wang, Preparation and electrochemical characterisation of polypyrrole-coated Li_2SnO_3 anode materials for lithium-ion batteries, Micro and Nano Letters 7 (2012) 1278–1281.

[27] Y. Zhao, Y. Huang, Q. Wang, X.Y. Wang, M. Zong, Carbon-doped Li_2SnO_3/graphene as an anode material for lithium-ion batteries, Ceramics International 39 (2013) 1741–1747.

[28] Q.F. Wang, Y. Huang, J. Miao, Y. Zhao, W. Zhang, Y. Wang, Graphene-Supported Ce–SnS_2 Nanocomposite as Anode Material for Lithium-Ion Batteries, Journal of the American Ceramic Society 96 (2013) 2190–2196, http://dx.doi.org/10.1111/jace.12302.